

---

# Self-Supervised Learning from Non-Object Centric Images with a Geometric Transformation Sensitive Architecture

---

Taeho Kim

Department of Artificial Intelligence, Hanyang University  
bok3948@hanyang.ac.kr

## Abstract

Most invariance-based self-supervised methods rely on single object-centric images (e.g., ImageNet images) for pretraining, learning invariant representations from geometric transformations. However, when images are not object-centric, the semantics of the image can be significantly altered due to cropping. Furthermore, as the model learns geometrically insensitive features, it may struggle to capture location information. For this reason, we propose a Geometric Transformation Sensitive Architecture that learns features sensitive to geometric transformations, specifically four-fold rotation, random crop, and multi-crop. Our method encourages the student to learn sensitive features by using targets that are sensitive to those transforms via pooling and rotating of the teacher feature map and predicting rotation. Additionally, since training insensitively to multi-crop can capture long-term dependencies, we use patch correspondence loss to train the model sensitively while capturing long-term dependencies. Our approach demonstrates improved performance when using non-object-centric images as pretraining data compared to other methods that learn geometric transformation-insensitive representations. We surpass the DINO[Caron et al. [2021b]] baseline in tasks including image classification, semantic segmentation, detection, and instance segmentation with improvements of 6.1 *Acc*, 3.3 *mIoU*, 3.4 *AP<sup>b</sup>*, and 2.7 *AP<sup>m</sup>*. Code and pretrained models are publicly available at: <https://github.com/bok3948/GTSA>

## 1 Introduction

Invariance-based methods are one of the primary self-supervised learning approaches for computer vision. These methods learn to be insensitive to various transformations, such as rotations, flips, crops, color jittering, blurring, and random grayscale, which provide an inductive bias that helps with representation learning[Chen and He [2020], Bardes et al. [2022a], Zbontar et al. [2021]].

Augmentations employed in self-supervised learning methods can be divided into two categories: photometric transformations and geometric transformations. Photometric transformations, such as color jittering, Gaussian blurring, and grayscale conversion, involve changes to the appearance of an image, like color, brightness, or contrast. geometric transformations, including random crop, multi-crop, flip and rotation, deal with changes to the spatial configuration of the image.

In the case of pretraining with non-object centric image, Learning invariant features from crop-related geometric transformations can be problematic. This is because cropped views may not always depict the same object[Purushwalkam and Gupta [2020], Zhang et al. [2022]]. In contrast, object-centric images are less prone to such issues due to their inherent focus on specific objects, which remain semantically consistent across various augmentations. This explains the significant performance drop observed when applying invariant methods to non-object centric images[Purushwalkam and

Gupta [2020], El-Nouby et al. [2021]]. It also explains that, to obtain comparable results with curated datasets, a considerably larger amount of uncurated data is required[Goyal et al. [2021]].

Furthermore, when learning to be insensitive to geometric transformations, there is a risk of not capturing location information. Since dense prediction models have to learn covariant features rather than invariant ones, learning geometrically insensitive features may not be appropriate.

As mentioned earlier, learning geometric transformation-insensitive features may lead to noise in learning. However, these transforms can still be beneficial for representation learning since they prevent pathological training behavior and provide diversity in inputs [Chen et al. [2020]]. Therefore, we propose a method that learns sensitive features with respect to those transforms, rather than insensitive features.

To achieve this, we must provide a sensitive target during training. For instance, to create a target that is sensitive to cropping, we pool the overlapping region from the teacher’s feature map, which can be seen as cropping, and provide it to the student as a target. Additionally, to make the model sensitive to four-fold rotations, we rotate the target feature map to align it appropriately with the student input, and we include a prediction task to match the rotation value of the student’s input. We decided not to make the model sensitive to flips because doing so could cause a performance drop [Dangovski et al. [2022]].

Additionally, we use a patch correspondence loss in our approach. When learning invariant features through multi-crop inputs, it will encourage global-to-local correspondence[Caron et al. [2021b], Caron et al. [2021a]], resulting to capture long-term dependencies. Our model uses an additional loss that encourages correspondence between patch representations through feature distance, allowing us to capture long-term dependencies without explicitly learning invariant features.[Bardet et al. [2022b]] Unlike encouraging correspondence between randomly selected crops, our approach induces correspondence between those that are closer in feature space, inducing more accurate correspondence.

Our experiments shows that when using non-centric images as pretraining data, it is better to learn sensitive features rather than geometric transformation insensitive features. We outperformed DINO[Caron et al. [2021b]], which is the most similar model to ours but tends to learn only insensitive features, in various tasks including image classification, semantic segmentation, detection, and instance segmentation, with improvements of 6.1 *Acc*, 3.3 *mIoU*, 3.4 *AP<sup>b</sup>*, and 2.7 *AP<sup>m</sup>*.

## 2 Related Work

**Non-Contrative Learning** Non-contrastive learning methods aim to learn an invariant bias towards transformations by training on different views of the same image, without explicit negative samples[Garrido et al. [2022]]. In the absence of negative samples, non-contrastive learning methods employ various alternative approaches to prevent representation collapse. These include non-contrastive losses that minimize redundancy across embeddings[Bardet et al. [2022a], Zbontar et al. [2021]], clustering-based techniques that maximize the entropy of the average embedding[Caron et al. [2019], Caron et al. [2021a], Goyal et al. [2021], Assran et al. [2022]], centering and sharpening output features[Caron et al. [2021b]], and heuristic strategies utilizing asymmetric architectural design with stop-gradient, additional predictors, and momentum encoders[Richemond et al. [2020], Chen and He [2020], Tian et al. [2021b]]. Our method belongs to the non-contrastive learning category and adopts an asymmetric architectural design to prevent representation collapse.

**Self-Supervised Learning with Uncurated dataset** Several self-supervised pretraining methods have been proposed for uncurated datasets, such as the clustering-based method presented in [Caron et al. [2021a], Tian et al. [2021a]]. These methods have shown good performance even when using uncurated datasets, and [Goyal et al. [2021]] demonstrated the scalability of their method to larger datasets for increased performance. Additionally, [El-Nouby et al. [2021]] showed that, given sufficient iterations, even a small non-object centric dataset can yield results that are comparable to those obtained using a larger, highly curated dataset.

However, our approach differs from other methods that aim to adapt to uncurated datasets. While clustering-based techniques are used in these methods, they still learn invariant representations to augmentations, whereas our approach learns features that are sensitive to geometric transformations.

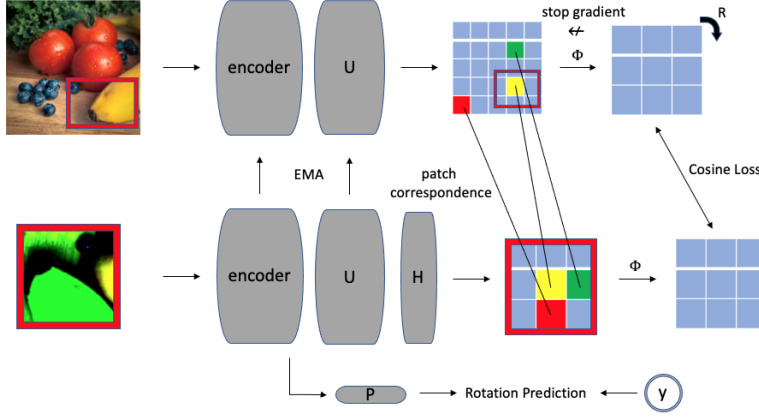


Figure 1: The GTSA. The Geometric Transformation Sensitive Architecture (GTSA). the teacher only receives global views only, while the student receives both global and local views. The learning process is designed to increase the similarity in overlapping regions and predicting four-fold rotation. Additionally, to capture long-term dependencies, GTSA encourages similarity between teacher patch representations and the student’s corresponding representations.

On the other hand, [Tian et al. [2021a]] aims to address the shift in the distribution of image classes rather than object-centric bias.

**Self-Supervised Methods that Learn sensitive to transforms** Intuitively, whether learning to be sensitive to transformations or not can be determined based on whether the model is trained to change its output in response to changes in the input. Early self-supervised learning methods, such as [Noroozi and Favaro [2017], Yamaguchi et al. [2021]], learned sensitive features by predicting the permutation or rotation applied to the input. As contrastive learning has gained prominence in representation learning, the significance of learning transformation-invariant representations has become increasingly evident [Misra and van der Maaten [2019], Chen et al. [2020], He et al. [2020]]. More recent work explore sensitive and insensitive features for representation learning. [Dangovski et al. [2022]] performance improvement has been achieved by learning features sensitive to four-fold rotation while insensitive to other transforms. Similarly, our model also learns to be sensitive to four-fold rotations and insensitive to other photometric transforms. However, our method additionally becomes sensitive to crop-related augmentations.

### 3 Methods

In this section, we describe the training procedure for our proposed GTSA method, as illustrated in Figure 1. We adopt an asymmetric Teacher-Student architecture, similar to those in Richmond et al. [2020] and Chen and He [2020]. The Teacher comprises an encoder and a projector, while the Student includes an encoder, projector, and predictor. Following the multi-crop strategy used in [Caron et al. [2021a], Caron et al. [2021b]], we feed only the global view to the Teacher and both global and local views to the Student. Our objectives involve maximizing the similarity between overlapping region representations and similar patch representations and predicting rotation.

**Inputs.** Similar to [Ziegler and Asano [2022]], we utilized various augmentation techniques including color jitter, random grayscale, random Gaussian noise, Gaussian blur, random resize crop, and multi-crop. Additionally, we employed four-fold rotation. For each image, we apply random augmentations and generate  $G$  global views and  $L$  local views. The inputs are  $[x_1^g, x_2^g, \dots, x_1^l, x_2^l, \dots]$ , where  $g$  and  $l$  indicate global and local view, respectively.  $x$  represents batchified images, and  $x \in \mathbb{R}^{B \times C \times H \times W}$ . Here,  $B$  is the batch size,  $C$  represents the number of image channels, and  $H$  and  $W$  denote the image size.

**Teacher and Student.** Apart from the additional predictor attached to the Student, the Teacher and Student share the same structural design. We utilized the ViT [Dosovitskiy et al. [2021]] as the

encoder and employed stacked CNN blocks for the projector, each block comprising a convolution layer, layer normalization[Ba et al. [2016]], GELU activation[Hendrycks and Gimpel [2020]] and residual connection[He et al. [2015]]. The predictor has a similar architecture to the projector but uses fewer CNN blocks in its composition. We annotated the Predictor and Projector as H and U, respectively. Note that both the projector and predictor do not reduce the spatial resolution of the encoder’s output. The Teacher does not get updated through gradient descent; instead, its weights follow the Student’s weights using exponential moving average.[Tarvainen and Valpola [2018], He et al. [2019]]

**Correspondence Region Pooling Operator.** We introduce a correspondence region pooling operator, denoted as  $\Phi(\cdot)$ . To be sensitive to crop-related augmentations, the student must receive a target that reflects the crop augmentation. The  $\Phi(\cdot)$  operator serves this purpose by cropping specific locations in the feature space. It extracts the overlapping portions between the teacher view and student view in the feature space using  $\Phi$ .

To accomplish this, we first calculate the overlap region bounding boxes in the input space and scale them to match the feature spatial resolution. We then apply the  $\Phi(\cdot)$  operator to both the student and teacher feature maps. We implement this operator using RoI-Align [He et al. [2018]].

**Rotation Operator.** To be sensitive to rotation, we propose a rotation operator. This operator rotates the teacher output feature map according to the input rotation. We denote this as  $R(\cdot)$ . By using this operator, the student receives a target that reflected the input rotation.

**Rotation Predictor.** As we employ the rotation prediction pretext task, we extract a vector from the student encoder output using a Global Average Pooling layer, as described by Lin et al. [2014]. This vector is then input into the rotation predictor, which generates logits for the rotation. The architecture of this process includes a linear layer, GELU activation, and a normalization layer. We denote the rotation predictor as P.

**Loss Function.** We denote the output feature map of the student predictor as  $z$  and the output feature map of the teacher’s projection layer as  $\tilde{z}$ .  $z \in \mathbb{R}^{B \times D \times h_s \times w_s}$  and  $\tilde{z} \in \mathbb{R}^{B \times D \times h_t \times w_t}$ , where  $B$  is the batch size,  $D$  is the feature dimension,  $h_s$  and  $w_s$  represent the spatial size of the student feature map, and  $h_t$  and  $w_t$  represent the spatial size of the teacher feature map. We apply  $\Phi$  to both  $z$  and  $\tilde{z}$ , and additionally apply  $R$  to  $\tilde{z}$ . We then compute the cosine similarity between them. The equation is as follows:

$$l(z, \tilde{z}) = -\frac{1}{B} \sum_{i=1}^B \frac{\Phi(z_i) \cdot R(\Phi(\tilde{z}_i))}{\|\Phi(z_i)\| \|R(\Phi(\tilde{z}_i))\|} \quad (1)$$

where  $i$  is the index of the batch, and the cosine similarity is calculated as the dot product of the two vectors divided by the product of their magnitudes.

For the Rotation prediction pretext task, we use rotation prediction loss, which is annotated with  $l_{rp}$ . We design this loss using cross-entropy loss. The equation is as follows:

$$l_{rp}(\mathbf{y}, \hat{\mathbf{y}}) = -\frac{1}{B} \sum_{i=1}^B \mathbf{y}_i \cdot \log \hat{\mathbf{y}}_i \quad (2)$$

where  $\mathbf{y}_i$  is the target indicating the  $i$ -th sample rotation angle.  $\hat{\mathbf{y}}_i$  is the Rotation Predictor output probability of the  $i$ -th sample. In this case, as we use four-fold rotation, the possible rotation angles are [0, 90, 180, 270] degrees.

Additionally, we use patch correspondence loss, which we annotate with  $l_{PC}$ . We pair semantically similar patches from the teacher and student patch representations based on their cosine similarity and make them more alike using the  $l_{PC}$  loss. Similar to [Bardes et al. [2022b]], we use cosine similarity to pair patches from the teacher and student representations. However, as noise may exist in this process, we do not encourage correspondence between all patches. Instead, we only encourage the similarity of the top- $K$  most similar features among all patches. This helps to ensure that we are aligning semantically similar patches while avoiding pairing patches that are too dissimilar.

Table 1: The iNaturalist 2019 image classification performance. performance was obtained by pretraining all models with 100 epochs on COCO train2017, followed by fine-tuning for 300 epochs using the same settings for all models.

Method	Top-1 Acc	Top-5 Acc
rand init	40.6	69.0
MoCo v3	48.8	76.3
DINO	54.8	82.9
GTSA (Ours)	<b>60.9</b>	<b>86.0</b>

$$l_{pc}(z, \tilde{z}) = -\frac{1}{B \times K} \sum_{i=1}^B \sum_{p=1}^K \frac{z_{i,p} \cdot \tilde{z}_{i,\tilde{p}}}{\|z_{i,p}\| \|\tilde{z}_{i,\tilde{p}}\|} \quad (3)$$

To consider multi-crop scenarios, we use the following total loss function:

$$\begin{aligned} \text{Loss} = & \frac{1}{G(L+G)-G} \sum_{\substack{g=1 \\ g \neq l}}^G \sum_{l=1}^{G+S} l(z_{g,l}, \tilde{z}_{g,l}) + \alpha * \frac{1}{G(L+G)-G} \sum_{\substack{g=1 \\ g \neq l}}^G \sum_{l=1}^{L+G} l_{pc}(z_{g,l}, \tilde{z}_{g,l}) \\ & + \beta * \frac{1}{L+G} \sum_{l=1}^{L+G} l_{rp}(\mathbf{y}_l, \hat{\mathbf{y}}_l) \end{aligned} \quad (4)$$

Here,  $\alpha$  and  $\beta$  are hyperparameters that control the impact of  $l_{pc}$  and  $l_{rp}$ , respectively.  $L$  and  $S$  denote the total number of global views and local views, respectively.

## 4 Experiments

To demonstrate the effectiveness of GTSA in learning high-quality representations from non-object centric images, we pretrained our model on the COCO2017[Lin et al. [2015]], a dataset composed of non-object centric images. We then evaluated the performance of our model by fine-tuning it on various downstream tasks, specifically Classification, Detection, Instance Segmentation, and Semantic Segmentation.

Additionally, we pretrained our model on the ADE20K[Zhou et al. [2018]] dataset, which also consists of non-object centric images. However, due to the larger size of other downstream task datasets compared to the pretraining dataset, we limited our evaluation to Semantic Segmentation on the ADE20K dataset.

**Baseline.** We chose Dino and MoCo v3[Chen et al. [2021]] as our baseline methods. These methods are highly relevant to our research as they, like us, employ the Vision Transformer (ViT) as an encoder and focus on learning insensitive features in a self-supervised manner. Thus, they provide a compelling counterpoint to our approach of learning sensitive features.

The official codes from these baseline methods were leveraged in producing our results. To ensure a fair and balanced comparison, all methods underwent pretraining under the same conditions: 100 pretraining epochs and the use of the ViT-S/16 encoder. Moreover, the fine-tuning process was executed in an entirely uniform manner across all methods.

**Implementation details.** We used the same hyperparameters as DINO, as much as possible. Specifically, we set the batch size to 512, the global view size to 224x224, and the local view size to 96x96. We also used a scheduler to start the momentum at 0.996, just like DINO, and gradually increased it to 1. For the optimizer, we employed AdamW[Loshchilov and Hutter [2019]] and set both /alpha and /beta to 0.5. Whether we pretrained using the ADE20K train dataset or the COCO train2017 dataset, we used exactly the same settings for pretraining. Our default model is ViT-S/16, and we pretrained it for 100 epochs."

Table 2: Evaluation of self-supervised pretraining with detection and instance segmentation. Performance was obtained by pretraining all models with 100 epochs on COCO train2017, followed by fine-tuning for a standard  $1 \times$  schedule using the same settings for all models.

Method	Detection			Instance Segmentation		
	$AP^b$	$AP^b_{50}$	$AP^b_{75}$	$AP^m$	$AP^m_{50}$	$AP^m_{75}$
rand init	23.2	42.3	22.5	23.0	40.0	23.3
MoCo v3	29.6	50.1	30.4	28.3	47.7	29.2
DINO	32.4	54.2	33.8	30.8	51.1	32.2
GTSA(ours)	<b>35.8</b>	<b>57.8</b>	<b>38.5</b>	<b>33.5</b>	<b>54.7</b>	<b>35.3</b>

Table 3: The ADE20K image semantic segmentation performance. Performance was obtained by pretraining all models with 100 epochs on COCO train2017, followed by fine-tuning for a standard 40K iteration schedule.

Method	aAcc	mIoU	mAcc
rand init	64.5	12.1	16.1
MoCo v3	72.7	23.5	31.7
DINO	74.7	27.3	35.9
GTSA (Ours)	<b>76.4</b>	<b>30.6</b>	<b>40.0</b>

**Image Classification.** We compared our method with other self-supervised methods in terms of image classification performance when fine-tuning on the iNaturalist 2019 dataset [Horn et al. [2018]]. Table 1 shows that our method outperforms other methods that learn geometric transformation invariant features. We achieve a 5.9 and 12.1 higher accuracy than DINO and MoCo-v3, respectively, and a 20.9 accuracy improvement compared to random initialization.

**Detection and Instance Segmentation.** Table 2 shows the performance of our method on COCO detection and instance segmentation tasks. GTSA outperforms DINO and MoCo-v3 by 3.4 and 6.2  $AP^b$  in detection, and by 2.7 and 5.2  $AP^m$  in instance segmentation, respectively. All models were fine-tuned using Mask R-CNN [He et al. [2018]] and FPN [Lin et al. [2017]] under the standard  $1 \times$  schedule.

**Semantic Segmentation.** Table 3 reports the performance of on ADE20K semantic segmentation using the Acc, mIoU, and mAcc metrics with all methods are pretrained with COCO train2017 dataset. While DINO achieves a 27.3 mIoU, GTSA attains a higher performance of 30.6 mIoU, which is a 3.3 mIoU improvement. Moreover, our method outperforms MoCo-v3 by 7.1 mIoU. All models were fine-tuned using Semantic FPN [Kirillov et al. [2019]] under the standard 40k iteration schedule, following the same approach as in [Yun et al. [2022]].

Table 4, also reports the performance of on ADE20K semantic segmentation but differ with in this table use ADE20K train dataset as pretraining data. GTSA outperforms DINO and MoCo with improvement 2.6 mIoU. fine-tuning setting are all same to Table 3.

## 5 Conclusion

We propose the Geometric Transformation Sensitive Architecture (GTSA) as a self-supervised method designed for non-object centric images. Our approach learns geometrically sensitive features by utilizing targets that reflect geometric transformations. Experimental results demonstrate that our method outperforms other transformation-invariant methods when pretrained on non-object centric images. In the future, we plan to explore the integration of Masked Image Modeling into our model.

## References

Mahmoud Assran, Mathilde Caron, Ishan Misra, Piotr Bojanowski, Florian Bordes, Pascal Vincent, Armand Joulin, Michael Rabbat, and Nicolas Ballas. Masked siamese networks for label-efficient learning, 2022.

Table 4: The ADE20K image semantic segmentation performance. Performance was obtained by pretraining all models with 100 epochs on ADE20K train dataset, followed by fine-tuning for a standard 40K iteration schedule.

Method	aAcc	mIoU	mAcc
rand init	64.5	12.1	16.1
MoCo v3	66.3	13.6	19.0
DINO	65.5	13.6	18.8
GTSA (Ours)	<b>67.0</b>	<b>16.2</b>	<b>22.4</b>

Jimmy Lei Ba, Jamie Ryan Kiros, and Geoffrey E. Hinton. Layer normalization, 2016.

Adrien Bardes, Jean Ponce, and Yann LeCun. Vicreg: Variance-invariance-covariance regularization for self-supervised learning, 2022a.

Adrien Bardes, Jean Ponce, and Yann LeCun. Vicregl: Self-supervised learning of local visual features, 2022b.

Mathilde Caron, Piotr Bojanowski, Armand Joulin, and Matthijs Douze. Deep clustering for unsupervised learning of visual features, 2019.

Mathilde Caron, Ishan Misra, Julien Mairal, Priya Goyal, Piotr Bojanowski, and Armand Joulin. Unsupervised learning of visual features by contrasting cluster assignments, 2021a.

Mathilde Caron, Hugo Touvron, Ishan Misra, Hervé Jégou, Julien Mairal, Piotr Bojanowski, and Armand Joulin. Emerging properties in self-supervised vision transformers, 2021b.

Ting Chen, Simon Kornblith, Mohammad Norouzi, and Geoffrey Hinton. A simple framework for contrastive learning of visual representations, 2020.

Xinlei Chen and Kaiming He. Exploring simple siamese representation learning. *2021 IEEE/CVF Conference on Computer Vision and Pattern Recognition (CVPR)*, pages 15745–15753, 2020.

Xinlei Chen, Saining Xie, and Kaiming He. An empirical study of training self-supervised vision transformers, 2021.

Rumen Dangovski, Li Jing, Charlotte Loh, Seungwook Han, Akash Srivastava, Brian Cheung, Pulkit Agrawal, and Marin Soljačić. Equivariant contrastive learning, 2022.

Alexey Dosovitskiy, Lucas Beyer, Alexander Kolesnikov, Dirk Weissenborn, Xiaohua Zhai, Thomas Unterthiner, Mostafa Dehghani, Matthias Minderer, Georg Heigold, Sylvain Gelly, Jakob Uszkoreit, and Neil Houlsby. An image is worth 16x16 words: Transformers for image recognition at scale, 2021.

Alaaeldin El-Nouby, Gautier Izacard, Hugo Touvron, Ivan Laptev, Hervé Jegou, and Edouard Grave. Are large-scale datasets necessary for self-supervised pre-training?, 2021.

Quentin Garrido, Yubei Chen, Adrien Bardes, Laurent Najman, and Yann Lecun. On the duality between contrastive and non-contrastive self-supervised learning, 2022.

Priya Goyal, Mathilde Caron, Benjamin Lefauveux, Min Xu, Pengchao Wang, Vivek Pai, Mannat Singh, Vitaliy Liptchinsky, Ishan Misra, Armand Joulin, and Piotr Bojanowski. Self-supervised pretraining of visual features in the wild, 2021.

Kaiming He, Xiangyu Zhang, Shaoqing Ren, and Jian Sun. Deep residual learning for image recognition, 2015.

Kaiming He, Georgia Gkioxari, Piotr Dollár, and Ross Girshick. Mask r-cnn, 2018.

Kaiming He, Haoqi Fan, Yuxin Wu, Saining Xie, and Ross B. Girshick. Momentum contrast for unsupervised visual representation learning. *2020 IEEE/CVF Conference on Computer Vision and Pattern Recognition (CVPR)*, pages 9726–9735, 2019.

- Kaiming He, Haoqi Fan, Yuxin Wu, Saining Xie, and Ross Girshick. Momentum contrast for unsupervised visual representation learning, 2020.
- Dan Hendrycks and Kevin Gimpel. Gaussian error linear units (gelus), 2020.
- Grant Van Horn, Oisin Mac Aodha, Yang Song, Yin Cui, Chen Sun, Alex Shepard, Hartwig Adam, Pietro Perona, and Serge Belongie. The inaturalist species classification and detection dataset, 2018.
- Alexander Kirillov, Ross Girshick, Kaiming He, and Piotr Dollár. Panoptic feature pyramid networks, 2019.
- Min Lin, Qiang Chen, and Shuicheng Yan. Network in network, 2014.
- Tsung-Yi Lin, Michael Maire, Serge Belongie, Lubomir Bourdev, Ross Girshick, James Hays, Pietro Perona, Deva Ramanan, C. Lawrence Zitnick, and Piotr Dollár. Microsoft coco: Common objects in context, 2015.
- Tsung-Yi Lin, Piotr Dollár, Ross Girshick, Kaiming He, Bharath Hariharan, and Serge Belongie. Feature pyramid networks for object detection, 2017.
- Ilya Loshchilov and Frank Hutter. Decoupled weight decay regularization, 2019.
- Ishan Misra and Laurens van der Maaten. Self-supervised learning of pretext-invariant representations, 2019.
- Mehdi Noroozi and Paolo Favaro. Unsupervised learning of visual representations by solving jigsaw puzzles, 2017.
- Senthil Purushwalkam and Abhinav Gupta. Demystifying contrastive self-supervised learning: Invariances, augmentations and dataset biases, 2020.
- Pierre H. Richemond, Jean-Bastien Grill, Florent Alth’e, Corentin Tallec, Florian Strub, Andrew Brock, Samuel L. Smith, Soham De, Razvan Pascanu, Bilal Piot, and Michal Valko. Byol works even without batch statistics. *ArXiv*, abs/2010.10241, 2020.
- Antti Tarvainen and Harri Valpola. Mean teachers are better role models: Weight-averaged consistency targets improve semi-supervised deep learning results, 2018.
- Yonglong Tian, Olivier J. Henaff, and Aaron van den Oord. Divide and contrast: Self-supervised learning from uncurated data, 2021a.
- Yuandong Tian, Xinlei Chen, and Surya Ganguli. Understanding self-supervised learning dynamics without contrastive pairs, 2021b.
- Shin’ya Yamaguchi, Sekitoshi Kanai, Tetsuya Shioda, and Shoichiro Takeda. Image enhanced rotation prediction for self-supervised learning, 2021.
- Sukmin Yun, Hankook Lee, Jaehyung Kim, and Jinwoo Shin. Patch-level representation learning for self-supervised vision transformers, 2022.
- Jure Zbontar, Li Jing, Ishan Misra, Yann LeCun, and Stéphane Deny. Barlow twins: Self-supervised learning via redundancy reduction. In *International Conference on Machine Learning*, 2021.
- Tong Zhang, Congpei Qiu, Wei Ke, Sabine Süssstrunk, and Mathieu Salzmann. Leverage your local and global representations: A new self-supervised learning strategy, 2022.
- Bolei Zhou, Hang Zhao, Xavier Puig, Tete Xiao, Sanja Fidler, Adela Barriuso, and Antonio Torralba. Semantic understanding of scenes through the ade20k dataset, 2018.
- Adrian Ziegler and Yuki M. Asano. Self-supervised learning of object parts for semantic segmentation, 2022.